

Carrier dynamics of Mg-doped indium nitride

H. Ahn, K.-J. Yu, Y.-L. Hong, and S. Gwo

Citation: *Applied Physics Letters* **97**, 062110 (2010); doi: 10.1063/1.3479523

View online: <http://dx.doi.org/10.1063/1.3479523>

View Table of Contents: <http://scitation.aip.org/content/aip/journal/apl/97/6?ver=pdfcov>

Published by the [AIP Publishing](#)

Articles you may be interested in

[Sulfur passivation of surface electrons in highly Mg-doped InN](#)

J. Appl. Phys. **114**, 103702 (2013); 10.1063/1.4820483

[Infrared to vacuum-ultraviolet ellipsometry and optical Hall-effect study of free-charge carrier parameters in Mg-doped InN](#)

J. Appl. Phys. **113**, 013502 (2013); 10.1063/1.4772625

[Erratum: "Carrier recombination processes in Mg-doped N-polar InN films" \[*Appl. Phys. Lett.* 98, 181908 \(2011\)\]](#)

Appl. Phys. Lett. **99**, 089901 (2011); 10.1063/1.3628458

[Carrier recombination processes in Mg-doped N-polar InN films](#)

Appl. Phys. Lett. **98**, 181908 (2011); 10.1063/1.3586775

[Vacancy-type defects in Mg-doped InN probed by means of positron annihilation](#)

J. Appl. Phys. **105**, 054507 (2009); 10.1063/1.3075907



NEW! Asylum Research MFP-3D Infinity™ AFM
Unmatched Performance, Versatility and Support

OXFORD INSTRUMENTS
The Business of Science®

Stunning high performance

Simpler than ever to GetStarted™

Widest range of accessories for materials science and bioscience

Comprehensive tools for nanomechanics

Carrier dynamics of Mg-doped indium nitride

H. Ahn,^{1,a)} K.-J. Yu,¹ Y.-L. Hong,² and S. Gwo²

¹Department of Photonics and Institute of Electro-Optical Engineering, National Chiao Tung University, Hsinchu 30010, Taiwan

²Department of Physics, National Tsing Hua University, Hsinchu 30013, Taiwan

(Received 24 May 2010; accepted 22 July 2010; published online 12 August 2010)

Recently, we have reported a significant enhancement (>500 times in intensity) in terahertz emission from Mg-doped indium nitride (InN:Mg) films compared to undoped InN. It was found that the intensity of terahertz radiation strongly depends on the background electron density. In this letter, we present the results on ultrafast time-resolved reflectivity measurement employed to investigate the carrier dynamics of InN:Mg. We find that the decay time constant of InN:Mg depends on background electron density in the same way as terahertz radiation does. The spatial redistribution of carriers in diffusion and drift is found to be responsible for the recombination behavior as well as terahertz radiation. © 2010 American Institute of Physics.

[doi:10.1063/1.3479523]

Due to its high electron affinity, as-grown indium nitride (InN) film is typically *n*-type and the realization of *p*-type InN is known to be difficult. Although there is still a lack of direct measurement results of hole transport, it has been proposed that the realization of *p*-type InN may be possible by using Mg as an acceptor dopant.¹ Recently, we have demonstrated a significant enhancement of terahertz emission from Mg-doped InN (InN:Mg). The emission mechanism was found to be dominated by the competition between drift and diffusion currents, depending on the background *n*-type carrier density (*n*).² In addition to the carrier density, terahertz emission depends on the spatial redistribution of carriers, including both background and photoexcited carriers.³ Therefore, it is essential to clarify the details of carrier dynamics in order to fully understand the terahertz emission mechanism. There have been several reports on the carrier dynamics of InN films^{4–12} and nanostructures,^{13,14} which discussed mostly on the ultrafast carrier dynamics of undoped InN. Although there was a report on Si-doped InN,¹⁰ no systematic study has been reported on carrier dynamics of InN:Mg and the contribution of background carriers. In order to identify the contribution of background electrons in carrier dynamics of InN, we performed the time-resolved optical reflectivity measurement on InN:Mg films grown with different Mg-doping levels. Experimental analysis demonstrates that band gap renormalization (BGR) and band filling (BF) processes dominate the initial time dependence of reflectivity. The time constant of hot-carrier cooling in InN:Mg was measured to be in the range of subpicosecond to a few picoseconds, which agrees with previous results.^{4–7,9–11} Meanwhile, the carrier decay time of InN:Mg shows a strong dependence on the background carrier density and its dependence is found to be similar to that of terahertz radiation. This phenomenon can be understood that the spatial redistribution of carriers not only determines terahertz emission but also influences the carrier decay process in InN:Mg.

Wurtzite *N*-polar, undoped, and Mg-doped InN films with different electron concentrations were grown by

plasma-assisted molecular beam epitaxy on Si(111). The film thicknesses of samples are in the range of 1–1.5 μm . Mg doping was performed with a high-purity Mg (6N) Knudsen cell and the Mg doping level was controlled by regulating the cell temperature between 180 and 270 °C. The electron concentration and mobility of each sample were determined by room-temperature Hall effect measurements. The optical pump-probe measurement was performed using a Ti:sapphire laser system, which delivers ~ 150 fs optical pulses at a center wavelength of 800 nm. The pump laser beam was incident on the samples at a near-normal angle and the transient reflectivity change ($\Delta R/R$) of the probe beam incident at 45° was recorded as a function of the delay time between the pump and probe pulses. Terahertz radiation was measured by using a time-domain terahertz measurement method and the details of experiment can be found elsewhere.² Near-infrared photoluminescence (PL) was measured at room temperature by a 1/4-m spectrometer equipped with a 600 g/mm grating.

Figure 1(a) shows the transient reflectivity of the undoped InN film measured at various excitation fluences (*F*) ranging from 100 to 500 $\mu\text{J}/\text{cm}^2$. The differential reflectivity $\Delta R/R$ of the samples excited at $F > 200$ $\mu\text{J}/\text{cm}^2$ sharply decreases with the pulse-width-limited falling time, which is much longer than the carrier-carrier scattering time (≤ 50 fs) measured by the terahertz time-domain spectroscopy method.¹⁵ The decreased differential reflectivity rapidly recovers to a positive value with a time constant of τ_1 and it is followed by a slow decay with a time constant of τ_2 . The maximum change in reflectivity $-(\Delta R/R)_{\text{max}}$ increases linearly with increasing pump fluence, indicating the contribution of intraband carrier absorption.

For photoexcited semiconductors, the temporal evolution of reflectivity can be affected by the carrier dynamics through several effects, such as BF, BGR, free carrier absorption, and carrier recombination.⁵ Among them, BGR due to the screening of electron–hole Coulomb interaction is the dominant process at high carrier density and its effect is shown as the decrease in reflectivity. Therefore, the initial sharp decrease in reflectivity observed in Fig. 1(a) indicates the strong contribution of BGR for highly photoexcited InN. As the photocarriers cool down and relax toward the band

^{a)}Author to whom correspondence should be addressed. Electronic mail: hyahn@mail.nctu.edu.tw.

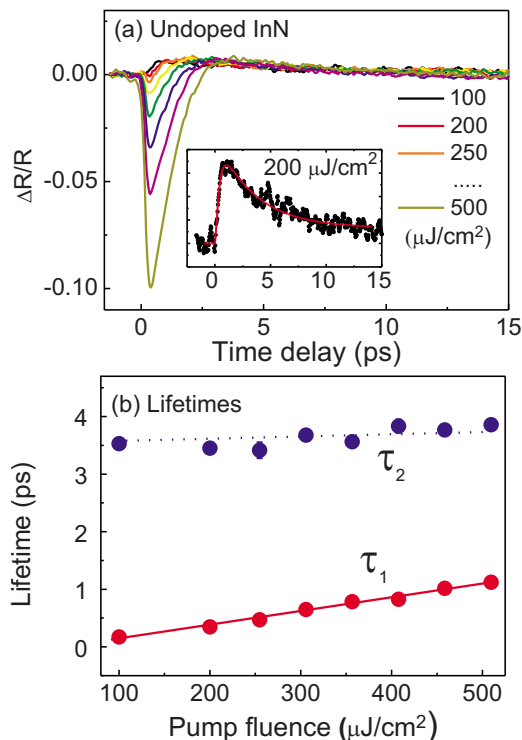


FIG. 1. (Color online) (a) Reflectivity transient of an undoped InN film with the background electron density of $3.1 \times 10^{18} \text{ cm}^{-3}$ measured under different levels of photoexcitation. After the initial pulse-width-limited sharp drop, the reflectivity recovers to positive values. Inset shows the transient reflectivity of the sample excited at the pump fluence of $200 \mu\text{J}/\text{cm}^2$ with the fitting result. (b) The carrier recovery (τ_1) and decay (τ_2) time constants obtained from the double exponential fits to the reflectivity responses shown in (a).

edge, the BF effect, which increases the reflectivity, begins to be important so that $\Delta R/R$ recovers toward less negative values. At low excitation ($F \leq 200 \mu\text{J}/\text{cm}^2$), due to the generation of less dense photocarriers, only the BF effect is observed, as shown in the inset in Fig. 1(a).

The carrier lifetimes τ_1 and τ_2 were obtained from the best fitting to the measured reflectivity using double exponential functions. Figure 1(b) shows that τ_1 increases linearly from ~ 0.2 to 1.2 ps as F increases from 100 to $500 \mu\text{J}/\text{cm}^2$, while τ_2 is nearly independent on the change in pump fluence. The slow decay of reflectivity can be affected by various processes, such as carrier diffusion, radiative, nonradiative, and Auger recombination. The pump fluence-independent τ_2 in Fig. 1(b) indicates that the carrier decay mechanism is not affected by radiative [$\propto(n+\Delta n)$] or Auger [$\propto(n+\Delta n)^2$] recombination process, but by the process which is independent on the total carrier density $n+\Delta n$, where n and Δn are the densities of background and photoexcited carriers, respectively.

In order to investigate the roles of Mg doping and the background carrier density in the carrier dynamics in InN, we measured the transient reflectivity of the InN:Mg films with various carrier densities. Each film was excited at the pump fluence of $350 \mu\text{J}/\text{cm}^2$. While the overall trend of transient reflectivity of InN:Mg shown in Fig. 2 is similar to that of undoped InN in Fig. 1(a), τ_2 and the minimum value of $\Delta R/R$ of the InN:Mg films show a clear dependence on n as is summarized in Fig. 3. Especially, as n decreases, τ_2 in Fig. 3(b) increases and reaches the maximum value

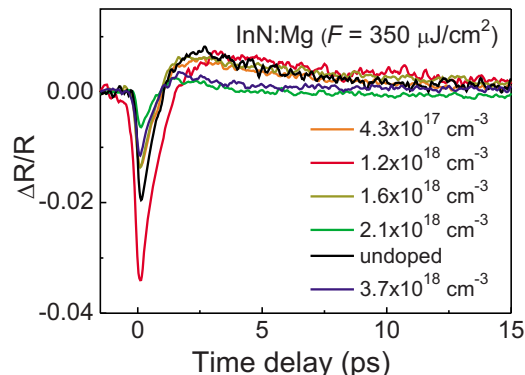


FIG. 2. (Color online) Reflectivity transient of the Mg-doped InN films under the photoexcitation of $350 \mu\text{J}/\text{cm}^2$. The background carrier densities of measured samples are $0.43 \times 10^{18} \text{ cm}^{-3}$, $1.2 \times 10^{18} \text{ cm}^{-3}$, $1.6 \times 10^{18} \text{ cm}^{-3}$, $2.1 \times 10^{18} \text{ cm}^{-3}$, and $3.7 \times 10^{18} \text{ cm}^{-3}$, respectively.

(~ 10 ps) at $n_c \sim 1 \times 10^{18} \text{ cm}^{-3}$. Further decrease in n below n_c results in the decrease in τ_2 . Figure 3(b) also shows that τ_1 of InN:Mg, corresponding to the cooling process, is nearly independent on the background carrier density. Photocarrier density-independent τ_2 in Fig. 1 suggests that the carrier decay process may be due to the defect-related nonradiative recombination.^{4,10} According to PL measurements on our InN:Mg films (not shown), PL intensity drastically decreases with the increasing Mg doping level, indicating the increase in defects. Therefore, one may expect a continuous decrease in the decay time with doping concentration. However, Fig. 3(b) shows that the decay time has an abnormal background carrier density dependence and this behavior cannot be described by the defect-related nonradiative recombination.

Interestingly, carrier density dependence of decay time in Fig. 3(b) resembles that of the terahertz radiation from the InN:Mg films, as shown in Fig. 3(c). In order to explain this

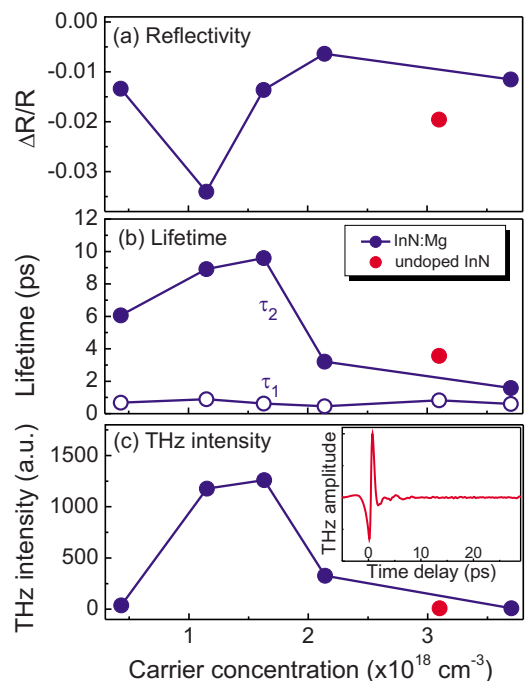


FIG. 3. (Color online) Carrier density dependence of differential reflectivity, carrier lifetimes, and terahertz radiation intensity of the InN:Mg film. Symbols at $n = 3.1 \times 10^{18} \text{ cm}^{-3}$ correspond to those of the reference undoped InN film. Inset shows a typical terahertz waveform.

resemblance, it is necessary to understand the terahertz emission mechanism of InN:Mg. With ultrafast photoexcitation, the spatial redistribution of electrons and holes can occur either by the diffusion field due to the difference in diffusion coefficients for electrons and holes or by the surface accumulation field attributed to the downward band bending by the Fermi level-pinning, whose relations are given by³

$$\frac{\partial \Delta n}{\partial t} \propto G + \frac{\partial}{\partial z} \left[D \frac{\partial \Delta n}{\partial z} \right] \pm \frac{\partial}{\partial z} [\mu_b E n] + [\mu_{ph} E \Delta n], \quad (1)$$

where μ_b and μ_{ph} correspond to the mobilities for background and photoexcited carriers, respectively, D denotes the diffusion coefficient, and G is the photoexcitation rate. Equation (1) shows that both background and photoexcited carriers participate in carrier redistribution through diffusion and drift. The ultrafast plasma oscillation under diffusion and drift fields gives rise to terahertz waves, which is heavily damped within 1 ps as shown in the inset of Fig. 3(c).

For highly photoexcited undoped InN, terahertz emission is dominated by carrier diffusion. But the strong Coulomb screening due to its exceptionally high background carrier density makes the terahertz emission from undoped InN small compared to that of other semiconductors, such as InAs. Recently, we have shown that doping InN with Mg can reduce the screening of the diffusion field and result in a dramatic enhancement of terahertz emission for InN:Mg with $n > n_c$.² We have also shown that for InN:Mg with a lower carrier density ($n < n_c$), terahertz emission is dominated by drift current which is formed in a region of the near-surface charge depletion layer and flows opposite to the diffusion current. In such case, intense terahertz radiation can be correlated with fast and large spatial separation of charged carriers. For largely separated electrons and holes, it may take much longer time to recombine to equilibrium after terahertz emission. Therefore, the measured recombination time constant reflects the spatial separation of charged carriers which is determined by the magnitude of terahertz field. And it explains the similar carrier density dependence of the decay time constant and the intensity of terahertz radiation shown in Figs. 3(b) and 3(c).

Finally, we assume the longest decay time constant of 10 ps for InN:Mg to be the time for electrons to diffuse through the penetration depth [$d \sim 133$ nm (Ref. 16)] under the screening-free diffusion field. The estimated longitudinal diffusion coefficient ($D_l \sim d^2 / \tau$) is 18 cm²/s, which is much

larger than in-plane diffusion coefficient of ~ 2 cm²/s on the surface measured by time-resolved transient grating spectroscopy.⁴

In summary, time-resolved reflectivity measurements have been used to determine the carrier dynamics of Mg-doped InN films. The initial time dependent behavior of reflectivity is dominated by the interplay between the effects of BGR and BF. The slow carrier decay time constant is found to be independent on the pump fluence but is dependent on the background carrier density. The similar background carrier density dependence between the decay time and the intensity of terahertz radiation for InN:Mg indicates that the spatial redistribution of electrons and holes due to drift and diffusion plays an important role in the recombination dynamics.

This work was supported in part by the National Science Council (NSC Grant No. 98-2112-M-009-009-MY3) and the ATU program of the Ministry of Education, Taiwan.

¹R. E. Jones, K. M. Yu, S. X. Li, W. Walukiewicz, J. W. Ager, E. E. Haller, H. Lu, and W. J. Schaff, *Phys. Rev. Lett.* **96**, 125505 (2006).

²H. Ahn, Y.-J. Yeh, Y.-L. Hong, and S. Gwo, *Appl. Phys. Lett.* **95**, 232104 (2009).

³K. Liu, J. Xu, T. Yuan, and X.-C. Zhang, *Phys. Rev. B* **73**, 155330 (2006).

⁴F. Chen, A. N. Cartwright, H. Lu, and W. J. Schaff, *Appl. Phys. Lett.* **87**, 212104 (2005).

⁵D. Zanato, N. Balkan, B. K. Ridley, G. Hill, and W. J. Schaff, *Semicond. Sci. Technol.* **19**, 1024 (2004).

⁶J. W. Pomeroy, M. Kuball, H. Lu, W. J. Schaff, X. Wang, and A. Yoshikawa, *Appl. Phys. Lett.* **86**, 223501 (2005).

⁷K. T. Tsen, J. G. Kiang, D. K. Ferry, H. Lu, W. J. Schaff, H.-W. Lin, and S. Gwo, *J. Phys.: Condens. Matter* **19**, 236219 (2007).

⁸T.-R. Tsai, C.-F. Chang, and S. Gwo, *Appl. Phys. Lett.* **90**, 252111 (2007).

⁹S.-Z. Sun, Y.-C. Wen, S.-H. Guo, H.-M. Lee, S. Gwo, and C.-K. Sun, *J. Appl. Phys.* **103**, 123513 (2008).

¹⁰R. Ascáubi, I. Wilke, S. Cho, H. Lu, and W. J. Schaff, *Appl. Phys. Lett.* **88**, 112111 (2006).

¹¹S. Nargelas, R. Aleckšiejunas, M. Vengris, T. Malinauskas, K. Jarasiunas, and E. Dimakis, *Appl. Phys. Lett.* **95**, 162103 (2009).

¹²K. Fukunaga, M. Hashimoto, H. Kunugita, J. Kamimura, A. Kikuchi, K. Kishino, and K. Ema, *Appl. Phys. Lett.* **95**, 232114 (2009).

¹³Y.-M. Chang and S. Gwo, *Appl. Phys. Lett.* **94**, 071911 (2009).

¹⁴A. Othonos, M. Zervos, and M. Pervolaraki, *Nanoscale Res. Lett.* **4**, 122 (2009).

¹⁵H. Ahn, Y.-P. Ku, C.-H. Chuang, C.-L. Pan, H.-W. Lin, Y.-L. Hong, and S. Gwo, *Appl. Phys. Lett.* **91**, 163105 (2007).

¹⁶H. Ahn, C.-H. Shen, C.-L. Wu, and S. Gwo, *Appl. Phys. Lett.* **86**, 201905 (2005).